PLOS ONE

RESEARCH ARTICLE

A high-throughput whole cell screen to identify inhibitors of *Mycobacterium tuberculosis*

Juliane Ollinger, Anuradha Kumar, David M. Roberts, Mai A. Bailey, Allen Casey, Tanya Parish*

Infectious Disease Research Institute, Seattle, Washington, United States of America

* Tanya.Parish@idri.org

Citation: Ollinger J, Kumar A, Roberts DM, Bailey MA, Casey A, Parish T (2019) A high-throughput whole cell screen to identify inhibitors of *Mycobacterium tuberculosis*. PLoS ONE 14(1): e0205479. https://doi.org/10.1371/journal.pone.0205479

Editor: Matthew Bogyo, Stanford University, UNITED STATES

Received: September 21, 2018

Accepted: December 4, 2018

Published: January 16, 2019

Data Availability Statement: The data underlying this study are available through the following link: https://pubchem.ncbi.nlm.nih.gov/bioassay/1259417.

Funding: The work at IDRI was funded in part by Eli Lilly and Company in support of the mission of the Lilly TB Drug Discovery Initiative. There was no additional external funding received for this study. The funders had no role in study design, data collection and analysis, decision to publish, or preparation of the manuscript.

Abstract

Tuberculosis is a disease of global importance for which novel drugs are urgently required. We developed a whole-cell phenotypic screen which can be used to identify inhibitors of *Mycobacterium tuberculosis* growth. We used recombinant strains of virulent *M. tuberculosis* which express far-red fluorescent reporters and used fluorescence to monitor growth *in vitro*. We optimized our high throughput assays using both 96-well and 384-well plates; both formats gave assays which met stringent reproducibility and robustness tests. We screened a compound set of 1105 chemically diverse compounds previously shown to be active against *M. tuberculosis* and identified primary hits which showed $\geq$ 90% growth inhibition. We ranked hits and identified three chemical classes of interest–the phenoxyalkylbenzamidazoles, the benzothiophene 1–1 dioxides, and the piperidinamines. These new compound classes may serve as starting points for the development of new series of inhibitors that prevent the growth of *M. tuberculosis*. This assay can be used for further screening, or could easily be adapted to other strains of *M. tuberculosis*.

Introduction

Tuberculosis (TB), caused by the bacterial pathogen *Mycobacterium tuberculosis*, is a disease of global importance which killed approximately 1.7 million people in 2016 [1]. A lengthy 4-drug regimen is used to treat active infection, but drug resistant strains have emerged and threaten efforts to control the disease. Multi-drug resistant (MDR) and extremely drug resistant (XDR) TB are gaining footholds in areas where HIV is predominant and/or antibiotic treatment of patients is administered incompletely or incorrectly [1]. Thus, there is an urgent need for new drugs that are effective at killing *M. tuberculosis* and which might shorten therapy.

High throughput screening of small molecules has the potential to identify new compound classes that are effective against *M. tuberculosis*. Biochemical screens have been used to find inhibitors of specific targets, normally essential enzymes. A number of targets have been tested [2–15] but this approach had limited success in finding hits with whole cell activity for a variety of reasons including lack of permeation, efflux, and poor target vulnerability or engagement [16].

Competing interests: Tanya Parish serves on the Editorial Board of PLOS ONE. This does not alter the authors' adherence to all the PLOS ONE policies on sharing data and materials.

In contrast, phenotypic screening relies on identifying compounds with whole cell activity from the outset, with no knowledge of the cellular target. Although there remain challenges in dealing with an organism which grows very slowly and requires handling within specialized containment facilities. A number of assays have been developed which use different approaches, for example the use of non-pathogenic surrogates such as *Mycobacterium tuberculosis H37Ra* [17], *Mycobacterium smegmatis* [18] or *Mycobacterium aurum* [19]. High throughput screening has been conducted with *M. tuberculosis* under a variety of conditions, including nutrient starvation [20], under multiple stresses [21, 22], or during infection of host cells [23, 24]. Assays using live cells are also available to determine disruption of specific pathways, such as ATP homeostasis [25], pH homeostasis [26], biofilm formation [27] or under specific conditions such as low oxygen [28].

Material and methods

Bacterial strains and growth conditions

M. tuberculosis H37Rv LP (ATCC 25618) [29] was grown in Middlebrook 7H9 medium supplemented with 10% v/v oleic acid, albumin, dextrose, catalase (OADC; Becton Dickinson), 0.05% w/v Tween 80 (7H9-OADC-Tw), and 50 μg/mL hygromycin (7H9-OADC-Tw-hyg), where required. Large scale cultures were grown in 100 mL of medium in 450 cm^2 roller bottles at 37˚C and 100 rpm. *M. tuberculosis* strain CHEAM3 and DREAM8 expressing codon-optimized mCherry and *Ds*Red from plasmids pCherry3 [30] and pBlazeC8 [31], respectively, were used.

Preparation of assay plates

Medium and compound was dispensed into sterile, black, 384-well, clear bottom plates (Greiner) using a Minitrak (Packard BioScience) with a 384-well head contained in a custom HEPA enclosure. Controls were 100 μM rifampicin in column 1 (final assay concentration of 2 μM rifampicin), DMSO in column 2 (final assay concentration 2%) and 125 nM rifampicin in column 23 (final assay concentration of 2.5 nM). *M. tuberculosis* culture was added to columns 1–23 using a MultiDrop Combi (Thermo Fisher); column 24 was not inoculated (contamination control).

Growth in plates

M. tuberculosis was grown to logarithmic phase (OD_{590} = 0.6–0.9) and filtered through a 0.5 μm cellulose-acetate membrane filter, diluted in fresh medium, and inoculated into 96-well or 384-well plates containing medium. Plates were incubated in plastic bags in a humidified incubator at 37˚C. OD and fluorescence were read using a Synergy 4 plate reader (BioTek) with excitation/emission of 586nm/614nm for mCherry and 560nm/590nm for *Ds*Red.

Data analysis

OD_{590} and fluorescence readouts were analyzed independently. The coefficient of variation (CV) was calculated as the standard deviation (StdDev) ÷ Mean. For each plate the minimum and maximum growth controls were used to determine the signal to background (S:B) ratio (calculated as MeanMaxSignal÷MeanMinSignal), signal to noise (S:N) ratio (calculated as (MeanMaxSignal-MeanMinSignal)÷StdDevMinSignal), and the Z-factor of the controls (1-((3*StdDevMaxSignal + 3*StdDevMinSignal)÷(MeanMaxSignal-MeanMinSignal)). For each well, the % inhibition was calculated with reference to the maximum growth control (DMSO only).

The complete data set is available at https://pubchem.ncbi.nlm.nih.gov/bioassay/1259417

Results and discussion

Assay development

We were interested in developing a simple whole cell screen which could be used in multiple formats to assess the anti-tubercular activity of large compound sets. We previously developed an assay to monitor growth based on fluorescence and optical density using a strain of *M. tuberculosis* constitutively expressing the far-red reporter mCherry which was robust and reproducible in 96-well format [32]. In this study we used recombinant *M. tuberculosis* constitutively expressing either codon-optimized *Ds*Red or mCherry to develop a 384-well high throughput assay.

We determined the minimum inhibitory concentration (MIC) for rifampicin against the parental strain (H37Rv-LP; ATCC 25618) and both the fluorescent strains (CHEAM3 expressing mCherry from plasmid pCherry3, and DREAM8 expressing *Ds*Red from plasmid pBlazeC8). We used a 10-point, 2-fold serial dilution in independent experiments in 96-well plates. Growth inhibition was calculated compared to control wells (DMSO), and curves fit using the four-parameter Levenberg-Marqardt algorithm. For both strains, we calculated MICs using OD_{590} and fluorescence independently and observed that the MIC for rifampicin was equivalent to the parental strain H37Rv-LP strain (Table 1). MICs derived using fluorescence as a readout were equivalent to OD_{590}-derived values (Table 1). Once we had confirmed the equivalence of the three strains in 96-well plates, we determined key parameters for transferring the assay to higher throughput in 384-well plates.

Optimizing fluorescence measurements

We optimized a number of parameters and variables. We had previously determined the optimal parameters for measuring mCherry fluorescence [32]. For *Ds*Red, we ran a set of spectral scans varying the excitation wavelength from 540 nm to 565 nm with a fixed emission of 590 nm, and varying the emission wavelength from 580 to 630 nm with a fixed excitation of 558 nm (Fig 1A and 1B). The signal was optimal at a range of excitation wavelengths around 560 nm, while it peaked at the emission wavelength of 592nm. Based on these scans we selected excitation and emission wavelengths of 560nm and 590nm for *Ds*Red.

We tested the alternatives of bottom and top-read optics in the plate-reader. We compared the use of an external plate shaker or the integral plate shaker in the reader. We obtained the lowest signal to noise (S:N) ratio when plates were not shaken prior to reading and when fluorescence measurements were performed using the bottom optics on the plate reader.

Optimizing inoculum and growth conditions

Several additional assay parameters were tested in the 384-well plates to determine the final assay conditions; the inoculum concentration, and the number of days of incubation prior to measurement of *M. tuberculosis* growth were adjusted to minimize the assay volume while

Table 1. Determination of rifampicin activity against recombinant strains.

	MIC (nM)	
	(OD_{590})	(RFU)
H37Rv-LP	6.6 ± 2.5 (n = 85)	*na*
CHEAM3	7.5 ± 1.9 (n = 96)	6.8 ± 2.2 (n = 86)
DREAM8	7.1 ± 2.2 (n = 520)	6.9 ± 2.4 (n = 520)

MIC, the concentration required to inhibit growth by 90%; *na*, not applicable

https://doi.org/10.1371/journal.pone.0205479.t001

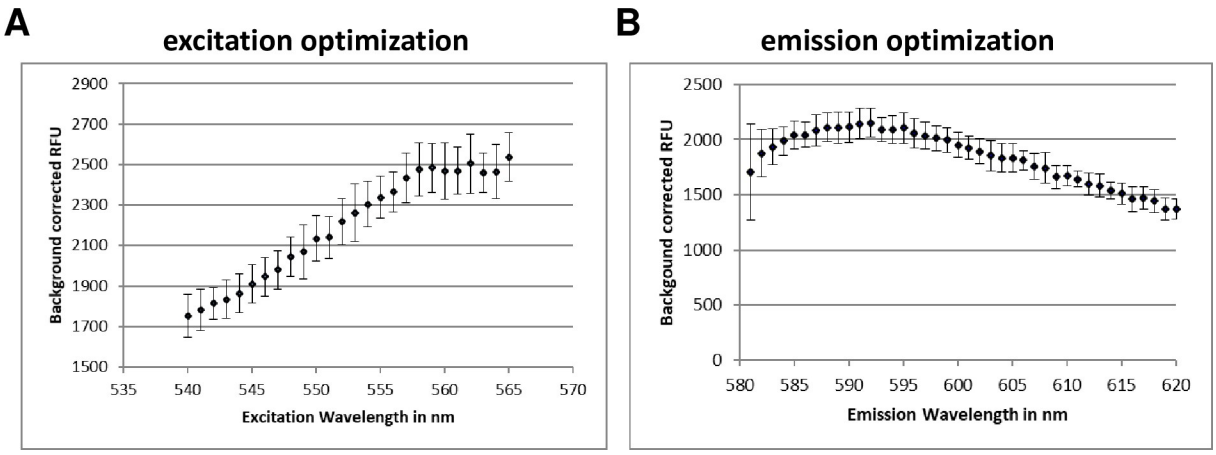

Fig 1. Optimization of fluorescence measurements. DREAM8 was dispensed into 384-well plates and fluorescence was measured at varying excitation wavelengths when the emission wavelength was fixed at 590nm **(A)** or at varying emission wavelengths when a fixed excitation of 558nm was used **(B)**. Data are the average ± SD from four wells.

https://doi.org/10.1371/journal.pone.0205479.g001

optimizing for signal and reproducibility. At a starting OD_{590} of 0.01, growth was still logarithmic between 4 and 5 days of incubation, whereas at a higher inoculum of OD_{590} = 0.05, cell growth plateaued at 5 days of growth (S1 Fig). To refine further we performed serial dilutions of CHEAM3 and monitored growth after five days of incubation. We measured fluorescence at the start of the experiment and on day 5 and calculated the S:B ratio (using the values obtained on day 0 of the experiment as the background) (Fig 2A). Wells with starting densities of 0.02–0.03 gave the highest S:B (Fig 2A). We ran a similar experiment using starting inocula of 0.01, 0.02 and 0.03 and incubated for 4 or 5 days, but we measured the ratio between full growth and complete inhibition using 2 μM rifampicin (Fig 2B); we found a higher ratio using OD_{590} of 0.02–0.03 (ratio of 13.0 and 13.8 respectively). However, variation was greater using

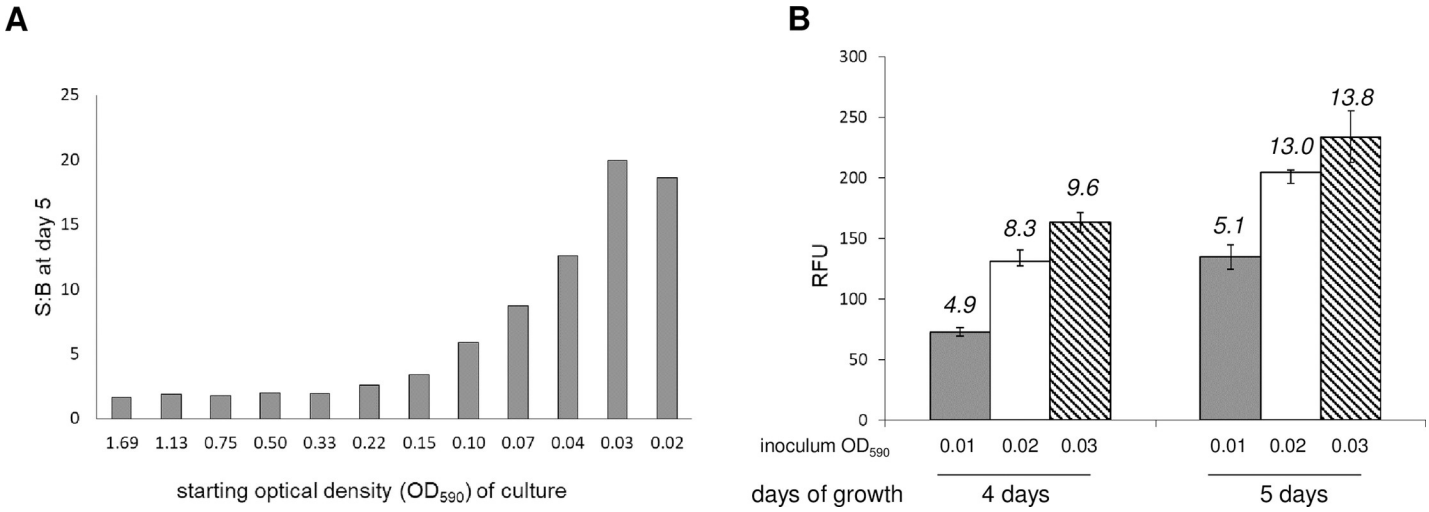

Fig 2. Optimization of growth conditions. (A) Serial dilutions of CHEAM3 were plated in triplicate in a 384 well plate and measured for fluorescence before and after five days of incubation. The signal to background (S:B) for each inoculum was calculated (average signal D0÷average signal D5) to identify the greatest amplitude to measure growth of cells over the course of 5 days. **(B)** 320 experimental wells of a 384 well plate were inoculated with CHEAM3 diluted to a starting OD_{590} of 0.01, 0.02 or 0.03. Plates were read on D4 and D5. The average fluorescence for each condition (n = 320) was plotted, with error bars indicating the standard deviation. The calculated signal to background (S:B) is shown above each bar.

https://doi.org/10.1371/journal.pone.0205479.g002

the larger inoculum of OD_{590} = 0.03, with a coeffeicient of variance (CV) of 9%, as compared to a CV of 5% for the inoculum at OD_{590} = 0.02. Thus a starting OD_{590} of 0.02 produced the best signal window and reproducibility in the 384-well assay.

Our final assay conditions were to inoculate 10 μL of *M. tuberculosis* at OD_{590} = 0.06 into 384-well plates prefilled with 20 μL of medium to give a final theoretical OD_{590} of 0.02. Plates were incubated for 5 days at 37˚C and both fluorescence and OD_{590} measured.

Validation of 384-well plate assay

Once the assay conditions were optimized, we assessed reproducibility according to NCGC guidelines [33]. Assay plates containing 20 μL of 7H9-Tw-OADC medium were prepared in a sterile environment. For validation, DMSO or test compounds were added to wells and the plates were inoculated with 10 μL of *M. tuberculosis* at an OD_{590} of 0.06. The final volume in each well was 30 μL, the final OD_{590} was 0.02, and the final concentration of DMSO in each well was 2%. Plates were incubated for five days at 37˚C in a humidified incubator. The plate layout was arranged as 320 sample wells in columns 3–22. The remaining four columns were reserved for plate controls: Column 1—minimum signal (2 μM rifampicin); Column 2—maximum signal (DMSO); Column 23—midpoint signal (2.5 nM rifampicin); Column 24 –contamination control (medium only, no inoculum). To test assay reproducibility, we ran a set of six plates independently on three days; two plates of minimum signal, two plates of maximum signal and two plates of midpoint signal (Fig 3). The % growth in each well was calculated with reference to the maximum signal (Column 2).

For each strain 2 plates containing maximum signal (Max = *M. tuberculosis* grown with 2% DMSO), mid signal (Mid = *M. tuberculosis* grown in the presence of 2.5 nM rifampicin), and minimum signal (Min = *M. tuberculosis* in the presence of 2 μM rifampicin) were run on three separate days. Max and Min controls (n = 16) from within each plate were used to calculate the signal to noise ratio (S:N), signal to background ratio (S:B), and Z-factor (measure of assay robustness as defined earlier). Intraplate controls were also used to calculate the % growth in each well. For the 320 sample wells in each individual plate the average signal, percent coefficient of variance (% CV) of the signal, and average % growth were calculated. The assay statistics generated to validate these two high throughput screens are shown in Table 2A and 2B.

The Z-factor, an indication of the robustness of the assay [34] was ≥ 0.7 in all plates. S:N was > 100 for both strains and S:B was ≥ 12 for *Ds*Red and ≥ 10 for mCherry. The CV was $< 20\%$ in all plate. The average mid-point signal did not vary more than 1.5-fold within a run or across the three runs. Thus, both assays passed statistical validation.

High throughput screen

To examine the performance of our high-throughput assay, we tested a set of compounds with known activity against *M. tuberculosis*. The Tuberculosis Antimicrobial Acquisition and Coordinating Facility (TAACF) at the Southern Research Institute (SRI) screened libraries containing over 300,000 compounds to identify inhibitors of *M. tuberculosis* growth [35, 36]. From the hits identified in these two screens a diversity set of 1105 compounds was obtained from the Division of Microbiology and Infectious Disease (DMID) at the National Institute of Allergy and Infectious Diseases (NIAID) as a library of potential anti-tubercular agents for the further development of *M. tuberculosis* drug development assays [37]. We obtained this set of compounds and tested them in both HTS-validated assays.

Compounds were obtained in plates, diluted to 0.35 mg/mL and transferred directly into assay plates to yield a final assay concentration of 7 μg/mL (final concentration of 2% DMSO). The standard assay conditions were used for each strain and % growth inhibition was plotted

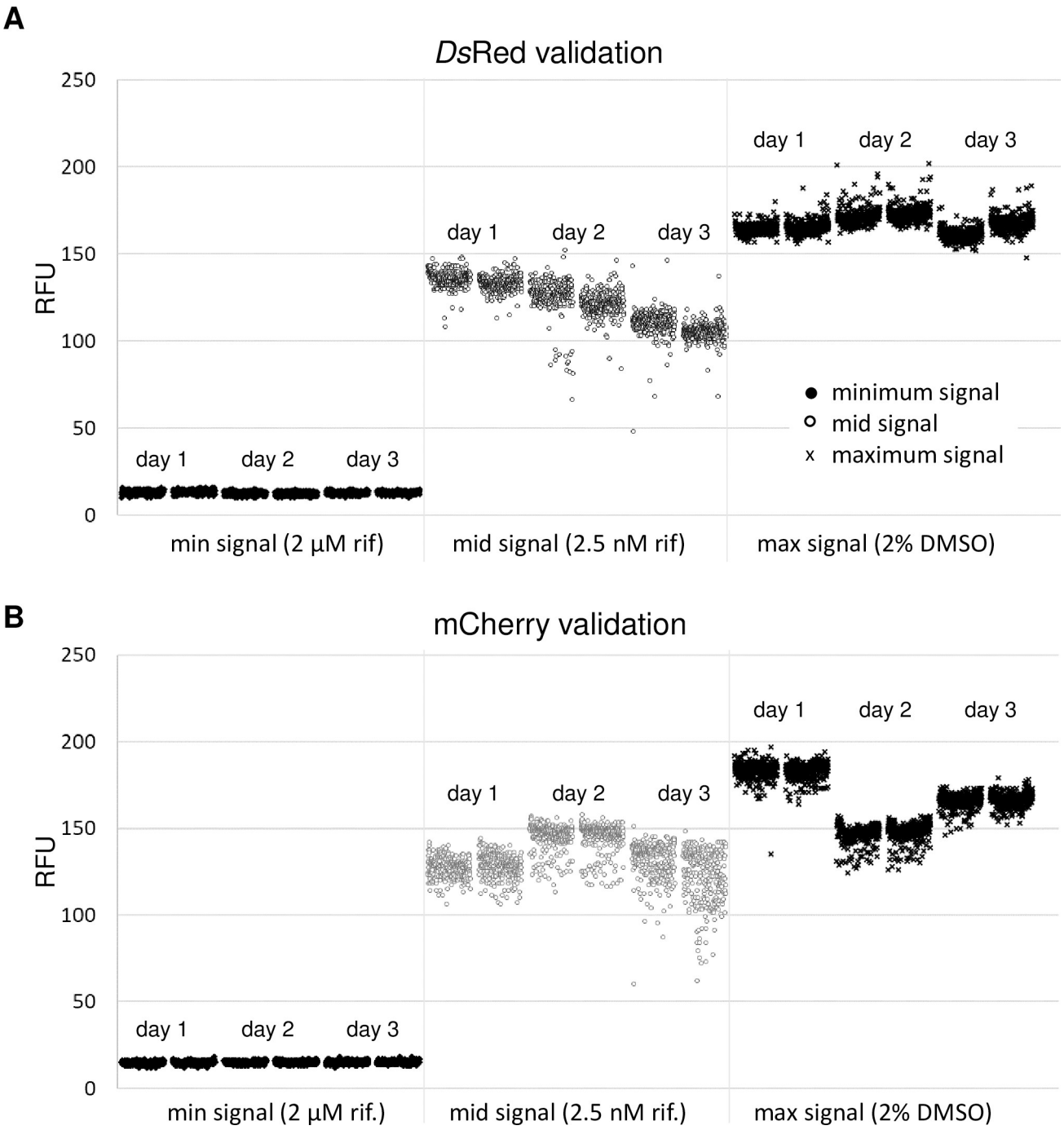

Fig 3. High throughput screen validation scatter plots: Two plates each containing minimum, midpoint, and maximum signal controls were run in 384-well plates on three separate days using the final assay conditions. Recombinant *M. tuberculosis* expressing **(A)** *Ds*Red or **(B)** mCherry was grown for 5 days. Relative fluorescence units (RFU) were measured in each well.

https://doi.org/10.1371/journal.pone.0205479.g003

(Fig 4A and 4B). Because the average of the maximum growth controls in each plate (n = 16) were used to calculate the % inhibition, any test well in which the fluorescence signal was higher than the control mean would be calculated as having negative inhibition. The Pearson coefficient, a statistical measurement of correlation between two data sets, was calculated for

Table 2. High throughput screen validation statistics.

A. DREAM8 validation

			intra-plate controls					
Signal	**Day**	**Plate**	**S:N**	**S:B**	**Z'**	**Avg Signal (RFU)**	**% CV**	**% growth**
Max	1	1	169	13	0.90	12.8	6.9	-0.4
Max	1	2	261	13	0.89	12.8	6.5	-0.4
Max	2	1	189	14	0.93	13.0	8.4	-0.1
Max	2	2	127	14	0.91	13.4	7.8	0.3
Max	3	1	119	14	0.87	12.5	7.8	0.0
Max	3	2	187	15	0.83	12.3	7.4	0.1
Mid	1	1	179	13	0.89	110.6	6.4	60.7
Mid	1	2	250	13	0.88	105.1	4.7	58.3
Mid	2	1	244	12	0.93	135.8	3.3	79.2
Mid	2	2	106	12	0.92	132.8	3.2	78.4
Mid	3	1	226	14	0.90	126.1	7.8	69.8
Mid	3	2	187	14	0.87	121.4	5.2	68.0
Min	1	1	178	13	0.88	161.2	2.1	97.3
Min	1	2	172	13	0.86	167.9	2.7	96.6
Min	2	1	136	12	0.87	164.8	1.7	97.0
Min	2	2	167	12	0.94	165.4	2.3	97.6
Min	3	1	180	13	0.86	171.5	2.8	99.2
Min	3	2	149	14	0.85	173.3	2.7	97.0

B. CHEAM3 validation

			intra-plate controls					
Signal	**Day**	**Plate**	**S:N**	**S:B**	**Z'**	**Avg Signal (RFU)**	**% CV**	**% growth**
Max	1	1	169	12	0.89	14.6	6.5	0.0
Max	1	2	161	12	0.87	14.8	6.5	0.1
Max	2	1	200	11	0.79	14.8	6.0	-0.3
Max	2	2	186	11	0.70	15.0	6.1	-0.4
Max	3	1	273	11	0.90	15.1	6.2	-0.1
Max	3	2	175	11	0.88	15.1	6.4	-0.2
Mid	1	1	245	12	0.88	127.2	4.5	63.4
Mid	1	2	172	12	0.79	128.2	5.3	63.9
Mid	2	1	167	10	0.80	145.1	5.0	90.7
Mid	2	2	177	10	0.75	144.9	5.6	90.5
Mid	3	1	150	11	0.91	131.1	7.7	77.3
Mid	3	2	247	10	0.90	122.5	12.3	68.1
Min	1	1	237	12	0.93	183.3	2.8	100.4
Min	1	2	206	12	0.86	183.1	2.5	99.7
Min	2	1	130	10	0.78	145.9	6.1	98.3
Min	2	2	137	10	0.75	147.6	3.7	101.2
Min	3	1	187	11	0.88	165.7	2.7	98.2
Min	3	2	249	11	0.88	166.6	2.5	97.6

https://doi.org/10.1371/journal.pone.0205479.t002

each strain. Fig 4A shows the replicate runs of CHEAM3 with a Pearson coefficient of r = 0.98 ($p<0.0001$). When DREAM8 was the strain used in the screen the correlation coefficient was r = 0.99 ($p<0.0001$) (Fig 4B). Thus the assay performed well in repeat runs with a large compound set.

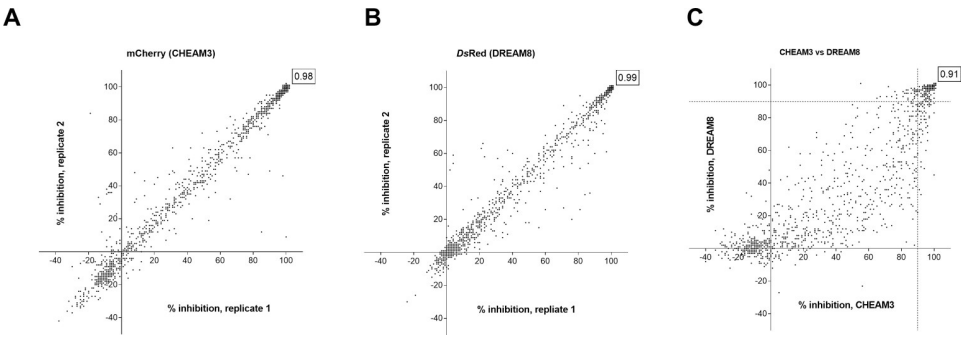

Fig 4. Small molecule compound library screen: A selected library of 1105 small molecules from NIH-SRI/TAACF was screened in replicate experiments against **(A)** CHEAM3 or **(B)** DREAM8. The % inhibition for each compound was calculated. The results from the first and second runs are plotted on the x- and y-axis, respectively, for both strains. For each strain the Pearson coefficient of linear correlation between the two replicate data sets was calculated in Graphpad Prism and is shown in boxed text in the upper right corner of each plot. **(C)** The average % inhibition of CHEAM3 and DREAM8 growth was calculated and plotted on the x- and y- axis, respectively. The calculated Pearson co-efficient comparing the data generated from the two different strains is shown in boxed text in the upper right corner of the plot.

https://doi.org/10.1371/journal.pone.0205479.g004

We compared the data between the two strains of *M. tuberculosis* strains (Fig 4C). There was a linear relationship between the two strains with a Pearson coefficient of r = 0.91. Thus, there was no statistical difference between the two strains.

Using CHEAM3, 470 compounds inhibited *M. tuberculosis* growth $\geq$ 80% while 169 compounds inhibited $\geq$ 99% (Fig 4A). Using DREAM8, 403 compounds inhibited $\geq$ 80% growth and 182 compounds inhibited $\geq$ 99% growth (Fig 4B). 377 compounds inhibited $\geq$ 80% growth in both strains. There were some minor differences between the two strains. 141 compounds showed $\geq$ 99% inhibition in both strains, with an additional 69 compounds with % I $\geq$ 99 in only one of the two strains (41 in DREAM8 and 28 in CHEAM3). However, of these 69 compounds 64 inhibited growth of the alternate strain by at least 90%. The hits from the screen were analysed and revealed three chemotypes of interest for further development: the phenoxyalkylbenzimidazoles (PAB), the benzothiophene 1–1 dioxides (BTD), and the piperidinamines (PIP). The other chemotypes in the library have been more thoroughly described in the two publications that first screened these molecules against *M. tuberculosis* [35, 36].

Discussion

We developed high throughput assays capable of screening large numbers of compounds using two fluorescent reporter strains of *M. tuberculosis*. We used both assays to screen a set of known compounds. Results from these assays were reproducible and the two strains yielded comparable results.

Only a fraction of the compounds we tested had activity against *M. tuberculosis* in our assays, even though these had previously been identified as active [35, 36]. A significant difference between the two screens is that we used a lower concentration of 7 μg/mL, as compared to 20 μg/ml previously used; thus we will only detect the more potent compounds. There are also some technical differences between the two assays, in particular that we used OD_{590} and fluorescence as a measure of increase in bacterial numbers, whereas the previous screen used Alamar Blue which monitors metabolic activity.

Using our fluorescent reporter strains, we identified 210 compounds that inhibited $\geq$ 99% growth, 141 of which inhibited $\geq$ 99% growth in both strains. We highlighted three chemotypes that were of interest to our group; the phenoxyalkylbenzimidazoles (PAB), benzothiophene 1–1 dioxides (BTD), and piperidinamines (PIP). We selected these chemical classes as

phenoxyalkylbenzimidazole (**PAB**)
MIC = 5.2 ± 1.5 μM (n=4)

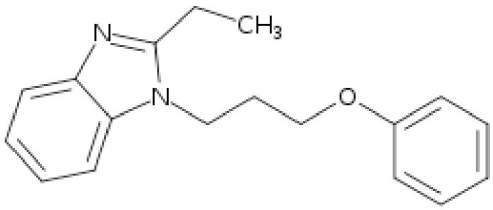

benzothiophene-1,1-dioxide (**BTD**)
MIC = 3.1 ± 0.07 μM (n=2)

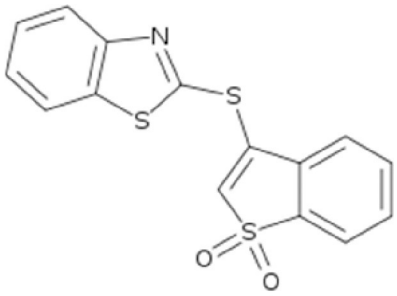

piperidinamine (**PIP**)
MIC = 9.9 ± 0.2 μM (n=2)

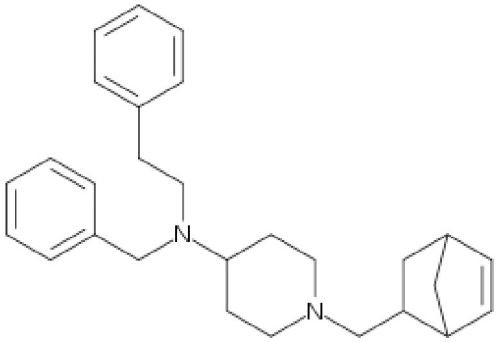

Fig 5. Selected hit compounds from screen. Three hit chemotypes identified in our screen were noted as being of interest for further development. Their structures and MICs are shown.

https://doi.org/10.1371/journal.pone.0205479.g005

being novel anti-mycobacterials and we (and others) have investigated these further in other publications pertaining to their recent characterization and development.

Compounds containing the benzimidazole core have long been known to have broad spectrum antibacterial activity [38, 39]. In the *M. tuberculosis* phenotypic screen performed by Ananthan et al., 88 compounds with the phenoxyalkylimidazole core were tested, PAB being the most potent active identified in this series, and the only compound in that study with benzimidazole substituted for the imidazole [35]. There have since been reports of benzimidazoles having activity against *M. tuberculosis* [40, 41]. We investigated this series and confirmed its potent activity and selectivity [42]. We have also shown that this class of compounds targets the electron transport chain, specifically targeting QcrB [43].

The benzothiophene 1–1 dioxides (BTD) series was also highlighted by Ananthan et al., as a chemotype. There were only a small number of analogs within this chemotype in their larger screen, all containing a thioether group at the 3-position and the most potent being the compound shown in Fig 5. They further noted that there were 40 additional compounds with the thiopene 1–1 dioxides lacking the benzene substitution in their primary screen, all of which

lacked activity. Using this as a starting point we explored the BTD series and evaluated their activity against *M. tuberculosis*. We were able to derive compounds that had good anti-tubercular activity (with MICs of 3–8 μM) but were unable to identify potent compounds analogs that were not cytotoxic to eukaryotic cells [44].

Some work has been done on piperidinamine-containing molecules as motilin-receptor agonists [45] and their clinical development for treating type 1 diabetes [46, 47]. Our screen identified the piperidinamines (PIP) as a potent chemotype. We obtained analogs within this chemotype that were commercially available and evaluated them for activity against *M. tuberculosis*, but none showed activity [48]. Based on our exploration of modifications around the piperidine core, we were unable to identify avenues for improved activity, and to our knowledge, the PIP chemotype has not yet further developed as an anti-tubercular agent.

In summary, we have developed and validated a robust whole cell phenotypic assay for *M. tuberculosis* in 384-well plates using one of two fluorescent reporters with equivalent outcomes. We used these assays to identify potent inhibitors of *M. tuberculosis* growth that have since proven to be interesting leads for drug development. This assay provides robust and reproducible results, and can be a core tool for high-throughput screening of large chemical libraries for the discovery of novel chemical entities to treat tuberculosis

Supporting information

S1 Fig. Preliminary study of M. tuberculosis growth conditions in 384-well plates. (A) CHEAM3 was diluted to an OD_{590} of 0.05 and 80 μL was plated in the wells of 384-well plates and incubated for 1, 2, 3, 5 or 6 days. Fluorescence was measured and the mean fluorescence from 192 wells (12 columns) is plotted along with error bars indicating the standard deviation **(B)** CHEAM3 was diluted to a theoretical OD_{590} of 0.01 and 30 μL was plated in the wells of 384 well plates. Plates were incubated for 3, 4 or 5 days. Fluorescence was measured in each well and the average fluorescence (n = 384) was plotted with error bars indicating the standard deviation.
(TIF)

Acknowledgments

This work was funded in part by Eli Lilly and Company in support of the mission of the Lilly TB Drug Discovery Initiative. There was no additional external funding received for this study.

Author Contributions

Conceptualization: Juliane Ollinger, Anuradha Kumar, David M. Roberts, Mai A. Bailey, Tanya Parish.

Data curation: Anuradha Kumar, David M. Roberts, Allen Casey, Tanya Parish.

Formal analysis: Juliane Ollinger, Anuradha Kumar, David M. Roberts, Tanya Parish.

Funding acquisition: Tanya Parish.

Investigation: Juliane Ollinger, David M. Roberts, Mai A. Bailey, Allen Casey, Tanya Parish.

Methodology: Juliane Ollinger, David M. Roberts, Mai A. Bailey, Allen Casey, Tanya Parish.

Resources: Tanya Parish.

Supervision: Juliane Ollinger, Anuradha Kumar, Allen Casey, Tanya Parish.

Validation: Juliane Ollinger, Anuradha Kumar, David M. Roberts, Mai A. Bailey, Allen Casey, Tanya Parish.

Writing – original draft: Anuradha Kumar, Tanya Parish.

Writing – review & editing: Juliane Ollinger, Anuradha Kumar, David M. Roberts, Mai A. Bailey, Allen Casey, Tanya Parish.

References

1. World Health Organization. Global tuberculosis report 2017.
2. Galandrin S, Guillet V, Rane RS, Leger M, N R, Eynard N, et al. Assay development for identifying inhibitors of the mycobacterial FadD32 activity. J Biomolec Screen. 2013; 18(5):576–87.
3. Geist JG, Lauw S, Illarionova V, Illarionov B, Fischer M, Grawert T, et al. Thiazolopyrimidine inhibitors of 2-methylerythritol 2,4-cyclodiphosphate synthase (IspF) from *Mycobacterium tuberculosis* and *Plasmodium falciparum*. ChemMedChem. 2010; 5(7):1092–101. https://doi.org/10.1002/cmdc.201000083 PMID: 20480490
4. Humnabadkar V, Jha RK, Ghatnekar N, De Sousa SM. A high-throughput screening assay for simultaneous selection of inhibitors of *Mycobacterium tuberculosis* 1-deoxy-D-xylulose-5-phosphate synthase (Dxs) or 1-deoxy-D-xylulose 5-phosphate reductoisomerase (Dxr). J Biomolec Screen. 2011; 16 (3):303–12.
5. Kumar A, Casey A, Odingo J, Kesicki EA, Abrahams G, Vieth M, et al. A high-throughput screen against pantothenate synthetase (PanC) identifies 3-biphenyl-4-cyanopyrrole-2-carboxylic acids as a new class of inhibitor with activity against *Mycobacterium tuberculosis*. PLOS One. 2013; 8(11):e72786. https://doi.org/10.1371/journal.pone.0072786 PMID: 24244263
6. Mann S, Eveleigh L, Lequin O, Ploux O. A microplate fluorescence assay for DAPA aminotransferase by detection of the vicinal diamine 7,8-diaminopelargonic acid. Anal Biochem. 2013; 432(2):90–6. https://doi.org/10.1016/j.ab.2012.09.038 PMID: 23068037
7. Simithy J, Reeve N, Hobrath JV, Reynolds RC, Calderon AI. Identification of shikimate kinase inhibitors among anti-*Mycobacterium tuberculosis* compounds by LC-MS. Tuberculosis. 2014; 94(2):152–8. https://doi.org/10.1016/j.tube.2013.12.004 PMID: 24429106
8. Anthony KG, Strych U, Yeung KR, Shoen CS, Perez O, Krause KL, et al. New classes of alanine racemase inhibitors identified by high-throughput screening show antimicrobial activity against *Mycobacterium tuberculosis*. PLOS One. 2011; 6(5):e20374. https://doi.org/10.1371/journal.pone.0020374 PMID: 21637807
9. Bhat J, Rane R, Solapure SM, Sarkar D, Sharma U, Harish MN, et al. High-throughput screening of RNA polymerase inhibitors using a fluorescent UTP analog. J Biomolec Screen. 2006; 11(8):968–76.
10. Gutierrez-Lugo MT, Baker H, Shiloach J, Boshoff H, Bewley CA. Dequalinium, a new inhibitor of *Mycobacterium tuberculosis* mycothiol ligase identified by high-throughput screening. Journal of biomolecular screening. 2009; 14(6):643–52. https://doi.org/10.1177/1087057109335743 PMID: 19525487
11. Sha S, Zhou Y, Xin Y, Ma Y. Development of a colorimetric assay and kinetic analysis for *Mycobacterium tuberculosis* D-glucose-1-phosphate thymidylyltransferase. J Biomolec Screen. 2012; 17(2):252–7.
12. Singh U, Sarkar D. Development of a simple high-throughput screening protocol based on biosynthetic activity of *Mycobacterium tuberculosis* glutamine synthetase for the identification of novel Inhibitors. J Biomolec Screen. 2006; 11(8):1035–42.
13. White EL, Southworth K, Ross L, Cooley S, Gill RB, Sosa MI, et al. A novel inhibitor of *Mycobacterium tuberculosis* pantothenate synthetase. J Biomolec Screen. 2007; 12(1):100–5.
14. Zhao N, Darby CM, Small J, Bachovchin DA, Jiang X, Burns-Huang KE, et al. Target-based screen against a periplasmic serine protease that regulates intrabacterial pH homeostasis in *Mycobacterium tuberculosis*. ACS Chem Biol. 2015; 10(2):364–71. https://doi.org/10.1021/cb500746z PMID: 25457457
15. Santa Maria JP Jr., Park Y, Yang L, Murgolo N, Altman MD, Zuck P, et al. Linking high-throughput screens to identify MOAs and novel inhibitors of *Mycobacterium tuberculosis* dihydrofolate reductase. ACS Chem Biol. 2017; 12(9):2448–56. https://doi.org/10.1021/acschembio.7b00468 PMID: 28806050
16. Payne DJ, Gwynn MN, Holmes DJ, Pompliano DL. Drugs for bad bugs: confronting the challenges of antibacterial discovery. Nature Rev Drug Disc. 2007; 6(1):29–40.
17. Gholap S, Tambe M, Nawale L, Sarkar D, Sangshetti J, Damale M. Design, synthesis, and pharmacological evaluation of fluorinated azoles as anti-tubercular agents. Archiv der Pharmazie. 2018; 351(2).

18. Cheng N, Porter MA, Frick LW, Nguyen Y, Hayden JD, Young EF, et al. Filtration improves the performance of a high-throughput screen for anti-mycobacterial compounds. PLOS One. 2014; 9(5):e96348. https://doi.org/10.1371/journal.pone.0096348 PMID: 24788852

19. Chung GA, Aktar Z, Jackson S, Duncan K. High-throughput screen for detecting antimycobacterial agents. Antimicrob Ag Chemother. 1995; 39(10):2235–8.

20. Grant SS, Kawate T, Nag PP, Silvis MR, Gordon K, Stanley SA, et al. Identification of novel inhibitors of nonreplicating *Mycobacterium tuberculosis* using a carbon starvation model. ACS Chem Biol. 2013; 8 (10):2224–34. https://doi.org/10.1021/cb4004817 PMID: 23898841

21. Deb C, Lee CM, Dubey VS, Daniel J, Abomoelak B, Sirakova TD, et al. A novel in vitro multiple-stress dormancy model for *Mycobacterium tuberculosis* generates a lipid-loaded, drug-tolerant, dormant pathogen. PLOS One. 2009; 4(6):e6077. https://doi.org/10.1371/journal.pone.0006077 PMID: 19562030

22. Gold B, Pingle M, Brickner SJ, Shah N, Roberts J, Rundell M, et al. Nonsteroidal anti-inflammatory drug sensitizes *Mycobacterium tuberculosis* to endogenous and exogenous antimicrobials. Proc Natl Acad Sci U S A. 2012; 109(40):16004–11. https://doi.org/10.1073/pnas.1214188109 PMID: 23012453

23. Brodin P, Poquet Y, Levillain F, Peguillet I, Larrouy-Maumus G, Gilleron M, et al. High content phenotypic cell-based visual screen identifies *Mycobacterium tuberculosis* acyltrehalose-containing glycolipids involved in phagosome remodeling. PLoS Pathogens. 2010; 6(9):e1001100. https://doi.org/10.1371/journal.ppat.1001100 PMID: 20844580

24. Christophe T, Ewann F, Jeon HK, Cechetto J, Brodin P. High-content imaging of *Mycobacterium tuberculosis*-infected macrophages: an in vitro model for tuberculosis drug discovery. Future Med Chem. 2010; 2(8):1283–93. https://doi.org/10.4155/fmc.10.223 PMID: 21426019

25. Mak PA, Rao SP, Ping Tan M, Lin X, Chyba J, Tay J, et al. A high-throughput screen to identify inhibitors of ATP homeostasis in non-replicating *Mycobacterium tuberculosis*. ACS Chem Biol. 2012; 7(7):1190–7. https://doi.org/10.1021/cb2004884 PMID: 22500615

26. Darby CM, Ingolfsson HI, Jiang X, Shen C, Sun M, Zhao N, et al. Whole cell screen for inhibitors of pH homeostasis in *Mycobacterium tuberculosis*. PLOS One. 2013; 8(7):e68942. https://doi.org/10.1371/journal.pone.0068942 PMID: 23935911

27. Wang F, Sambandan D, Halder R, Wang J, Batt SM, Weinrick B, et al. Identification of a small molecule with activity against drug-resistant and persistent tuberculosis. Proc Natl Acad Sci U S A. 2013; 110 (27):E2510–7. https://doi.org/10.1073/pnas.1309171110 PMID: 23776209

28. Cho SH, Warit S, Wan B, Hwang CH, Pauli GF, Franzblau SG. Low-oxygen-recovery assay for high-throughput screening of compounds against nonreplicating *Mycobacterium tuberculosis*. Antimicrob Ag Chemother. 2007; 51(4):1380–5.

29. Ioerger TR, Feng Y, Ganesula K, Chen X, Dobos KM, Fortune S, et al. Variation among genome sequences of H37Rv strains of *Mycobacterium tuberculosis* from multiple laboratories. J Bacteriol. 2010; 192(14):3645–53. https://doi.org/10.1128/JB.00166-10 PMID: 20472797

30. Carroll P, Schreuder LJ, Muwanguzi-Karugaba J, Wiles S, Robertson BD, Ripoll J, et al. Sensitive detection of gene expression in mycobacteria under replicating and non-replicating conditions using optimized far-red reporters. PLOS One. 2010; 5(3):e9823. https://doi.org/10.1371/journal.pone.0009823 PMID: 20352111

31. Carroll P, Muwanguzi J, Parish T. Optimization of the DsRed fluorescent protein for use in Mycobacterium tuberculosis. bioRxiv. 2018. https://doi.org/10.1101/383836

32. Ollinger J, Bailey MA, Moraski GC, Casey A, Florio S, Alling T, et al. A dual read-out assay to evaluate the potency of compounds active against *Mycobacterium tuberculosis*. PLOS One. 2013; 8(4):e60531. https://doi.org/10.1371/journal.pone.0060531 PMID: 23593234

33. Iversen PW, Beck B, Chen Y-F, Dere W, Devanarayan V, Eastwood BJ, et al. HTS Assay Validation. 2012. In: Assay Guidance Manual [Internet]. Eli Lilly & Company and the National Center for Advancing Translational Sciences. Available from: https://www.ncbi.nlm.nih.gov/books/NBK83783/.

34. Zhang JH, Chung TD, Oldenburg KR. A simple statistical parameter for use in evaluation and validation of high throughput screening assays. J Biomolec Screen. 1999; 4(2):67–73.

35. Ananthan S, Faaleolea ER, Goldman RC, Hobrath JV, Kwong CD, Laughon BE, et al. High-throughput screening for inhibitors of *Mycobacterium tuberculosis* H37Rv. Tuberculosis. 2009; 89(5):334–53. https://doi.org/10.1016/j.tube.2009.05.008 PMID: 19758845

36. Maddry JA, Ananthan S, Goldman RC, Hobrath JV, Kwong CD, Maddox C, et al. Antituberculosis activity of the molecular libraries screening center network library. Tuberculosis. 2009; 89(5):354–63. https://doi.org/10.1016/j.tube.2009.07.006 PMID: 19783214

37. Goldman RC, Laughon BE. Discovery and validation of new antitubercular compounds as potential drug leads and probes. Tuberculosis. 2009; 89(5):331–3. https://doi.org/10.1016/j.tube.2009.07.007 PMID: 19716767

38. He Y, Wu B, Yang J, Robinson D, Risen L, Ranken R, et al. 2-piperidin-4-yl-benzimidazoles with broad spectrum antibacterial activities. Bioorg Med Chem Lett. 2003; 13(19):3253–6. PMID: 12951103

39. Ozkay Y, Tunali Y, Karaca H, Isikdag I. Antimicrobial activity and a SAR study of some novel benzimidazole derivatives bearing hydrazone moiety. Eur J Med Chem. 2010; 45(8):3293–8. https://doi.org/10.1016/j.ejmech.2010.04.012 PMID: 20451306

40. Ojima I, Kumar K, Awasthi D, Vineberg JG. Drug discovery targeting cell division proteins, microtubules and FtsZ. Bioorg Med Chem. 2014; 22(18):5060–77. https://doi.org/10.1016/j.bmc.2014.02.036 PMID: 24680057

41. Gong Y, Somersan Karakaya S, Guo X, Zheng P, Gold B, Ma Y, et al. Benzimidazole-based compounds kill *Mycobacterium tuberculosis*. Eur J Med Chem. 2014; 75:336–53. https://doi.org/10.1016/j.ejmech.2014.01.039 PMID: 24556148

42. Chandrasekera NS, Alling T, Bailey MA, Files M, Early JV, Ollinger J, et al. Identification of Phenoxyalkylbenzimidazoles with Antitubercular Activity. J Med Chem. 2015; 58(18):7273–85. https://doi.org/10.1021/acs.jmedchem.5b00546 PMID: 26295286

43. Chandrasekera NS, Berube BJ, Shetye G, Chettiar S, O'Malley T, Manning A, et al. Improved phenoxyalkylbenzimidazoles with activity against *Mycobacterium tuberculosis* appear to target QcrB. ACS Infect Dis. 2017; 3(12):898–916. https://doi.org/10.1021/acsinfecdis.7b00112 PMID: 29035551

44. Chandrasekera NS, Bailey MA, Files M, Alling T, Florio SK, Ollinger J, et al. Synthesis and anti-tubercular activity of 3-substituted benzo[b]thiophene-1,1-dioxides. PeerJ. 2014; 2:e612. https://doi.org/10.7717/peerj.612 PMID: 25320680

45. Westaway SM, Brown SL, Fell SC, Johnson CN, MacPherson DT, Mitchell DJ, et al. Discovery of N-(3-fluorophenyl)-1-[(4-([(3S)-3-methyl-1-piperazinyl]methyl)phenyl)acetyl]-4-pi peridinamine (GSK962040), the first small molecule motilin receptor agonist clinical candidate. J Med Chem. 2009; 52(4):1180–9. https://doi.org/10.1021/jm801332q PMID: 19191554

46. Chapman MJ, Deane AM, O'Connor SL, Nguyen NQ, Fraser RJ, Richards DB, et al. The effect of camicinal (GSK962040), a motilin agonist, on gastric emptying and glucose absorption in feed-intolerant critically ill patients: a randomized, blinded, placebo-controlled, clinical trial. Crit Care. 2016; 20(1):232. https://doi.org/10.1186/s13054-016-1420-4 PMID: 27476581

47. Hellstrom PM, Tack J, Johnson LV, Hacquoil K, Barton ME, Richards DB, et al. The pharmacodynamics, safety and pharmacokinetics of single doses of the motilin agonist, camicinal, in type 1 diabetes mellitus with slow gastric emptying. Br J Pharmacol. 2016; 173(11):1768–77. https://doi.org/10.1111/bph.13475 PMID: 26924243

48. Chandrasekera NS, Alling T, Bailey M, Korkegian A, Ahn J, Ovechkina Y, et al. The 4-aminopiperidine series has limited anti-tubercular and anti-staphylococcus aureus activity. J Negat Results Biomed. 2015; 14:4. https://doi.org/10.1186/s12952-015-0024-x PMID: 25881065